IJC
International Journal of Cancer

Hsa-miR-139-5p is a prognostic thyroid cancer marker involved in HNRNPF-mediated alternative splicing

Cristina Montero-Conde[1]*, Osvaldo Graña-Castro[2], Guillermo Martín-Serrano[2], Ángel M. Martínez-Montes[1], Eduardo Zarzuela[3], Javier Muñoz[3], Rafael Torres-Perez[1], Guillermo Pita[4], Alfonso Cordero-Barreal[1], Luis J. Leandro-García[1], Rocío Letón[1], Isabel López de Silanes[5], Sonsoles Guadalix[6], Andrés Pérez-Barrios[7], Federico Hawkins[6], Almudena Guerrero-Álvarez[6], Cristina Álvarez-Escolá[8], Rita M. Regojo-Zapata[9], Bruna Calsina[1], Laura Remacha[1], Juan M. Roldán-Romero[1], María Santos[1], Javier Lanillos[1], Mireia Jordá[10], Garcilaso Riesco-Eizaguirre[11,12,13], Carles Zafon[14,15], Anna González-Neira[4], Maria A. Blasco[5], Fátima Al-Shahrour[2], Cristina Rodríguez-Antona[1], Alberto Cascón[1] and Mercedes Robledo[1,16]*

[1]Hereditary Endocrine Cancer Group, Spanish National Cancer Research Centre (CNIO), Madrid, Spain
[2]Bioinformatics Unit, Spanish National Cancer Research Centre (CNIO), Madrid, Spain
[3]Proteomics Core Unit and Proteored-ISCIII, Spanish National Cancer Research Centre (CNIO), Madrid, Spain
[4]CEGEN Unit, Spanish National Cancer Research Centre (CNIO), Madrid, Spain
[5]Telomeres and Telomerase Group, Spanish National Cancer Research Centre (CNIO), Madrid, Spain
[6]Endocrinology and Nutrition Department, Hospital Universitario 12 de Octubre, Madrid, Spain
[7]Anatomical Pathology Section, Hospital Universitario 12 de Octubre, Madrid, Spain
[8]Endocrinology and Nutrition Department, Madrid, Spain
[9]Anatomical Pathology Section Hospital Universitario La Paz, Madrid, Spain
[10]Program for Predictive and Personalized Medicine of Cancer, Germans Trias i Pujol Research Institute, Barcelona, Spain
[11]Endocrinology and Nutrition Department, Hospital Universitario de Móstoles, Madrid, Spain
[12]Biomedical Research Networking Centre in Oncology (CIBERONC), Institute of Health Carlos III, Madrid, Spain
[13]Universidad Francisco de Vitoria, Madrid, Spain
[14]Diabetes and Metabolism Research Unit and Endocrinology Department, Hospital Universitari Vall d'Hebron, Barcelona, Spain
[15]Biomedical Research Networking Centre on Diabetes and Associated Metabolic Diseases (CIBERDEM), Institute of Health Carlos III, Madrid, Spain
[16]Biomedical Research Networking Centre on Rare Diseases (CIBERER), Institute of Health Carlos III, Madrid, Spain

It is critical to identify biomarkers and functional networks associated with aggressive thyroid cancer to anticipate disease progression and facilitate personalized patient management. We performed miRNome sequencing of 46 thyroid tumors enriched with advanced disease patients with a median follow-up of 96 months. MiRNome profiles correlated with tumor-specific histopathological and molecular features, such as stromal cell infiltration and tumor driver mutation. Differential expression analysis revealed a consistent hsa-miR-139-5p downexpression in primary carcinomas from patients with recurrent/metastatic disease compared to disease-free patients, sustained in paired local metastases and validated in publicly

*C.M.C. and M.R. contributed equally to this work

Additional Supporting Information may be found in the online version of this article.

Key words: thyroid cancer, miRNome sequencing, stroma infiltration, hsa-miR139-5p and HNRNPF

Abbreviations: ATC: anaplastic thyroid carcinoma; DTC: differentiated thyroid carcinoma; FA: follicular adenoma; FTC: follicular thyroid carcinoma, a DTC sub-type; iTRAQ: isobaric tags for relative and absolute quantitation; NT: normal thyroid; PDTC: poorly differentiated thyroid carcinoma; PTC: papillary thyroid carcinoma, a DTC sub-type; rMATS: multivariate analysis of transcript splicing; SCS: stromal cell score; TC: thyroid carcinoma

Conflict of interest: The authors have declared that no conflict of interest exists.

Grant sponsor: CAM; **Grant numbers:** S2017/BMD-3724, TIRONET2-CM; **Grant sponsor:** Fundación Científica Asociación Española Contra el Cáncer; **Grant number:** AIO15152858; **Grant sponsor:** Instituto de Salud Carlos III (ISCIII), Acción Estratégica en Salud, cofinanciado a través del Fondo Europeo de Desarrollo Regional (FEDER); **Grant numbers:** PI14/00240, PI17/01796

DOI: 10.1002/ijc.32622

History: Received 29 Mar 2019; Accepted 30 Jul 2019; Online 12 Aug 2019

Correspondence to: Cristina Montero-Conde, Hereditary Endocrine Cancer Group, Spanish National Cancer Research Centre (CNIO), C/Melchor Fernández Almagro 3, 28029 Madrid, Spain, Tel.: +34-917-328-000, Fax: +34-912-246-911, E-mail: cmontero@cnio.es; or Mercedes Robledo, Hereditary Endocrine Cancer Group, Spanish National Cancer Research Centre (CNIO), C/Melchor Fernández Almagro 3, 28029 Madrid, Spain, Tel.: +34-917-328-000, Fax: +34-912-246-911, E-mail: mrobledo@cnio.es

available thyroid cancer series. Exogenous expression of hsa-miR-139-5p significantly reduced migration and proliferation of anaplastic thyroid cancer cells. Proteomic analysis indicated RICTOR, SMAD2/3 and HNRNPF as putative hsa-miR-139-5p targets in our cell system. Abundance of *HNRNPF* mRNA, encoding an alternative splicing factor involved in cryptic exon inclusion/exclusion, inversely correlated with hsa-miR-139-5p expression in human tumors. RNA sequencing analysis revealed 174 splicing events differentially regulated upon HNRNPF repression in our cell system, affecting genes involved in RTK/RAS/MAPK and PI3K/AKT/MTOR signaling cascades among others. These results point at the hsa-miR-139-5p/HNRNPF axis as a novel regulatory mechanism associated with the modulation of major thyroid cancer signaling pathways and tumor virulence.

What's new?

Recurrent or metastatic thyroid cancer generally leads to worse outcomes and higher mortality. To search for a prognostic marker in such cases, these authors sequenced the microRNA expression profile, or miRNome, of 46 thyroid samples. They compared differential expression between patients with recurrent/metastatic disease and those who remained cancer free over the 8-year follow-up. One miRNA, hsa-miR-139-5p, was associated with recurrent disease independent of genetic background. Expression of hsa-miR-139-5p, they found, influences expression of an alternative splicing factor, HNRNPF, which in turn controls the transcript balance of genes involved in key cancer-related pathways, a novel mechanism associated with tumor virulence.

Introduction

Around 15% of patients with differentiated thyroid carcinomas (DTCs) suffer distant metastases or recurrent disease. These patients frequently lose the ability to trap radioiodine (RAI) and present worse outcome with a substantially increased mortality (10-year survival rate of 10–30%).[1] Furthermore, dedifferentiated anaplastic and poorly differentiated thyroid cancers (ATCs and PDTCs, respectively) are RAI refractory and are mostly lethal within 5 years of follow-up.[2]

Aggressive thyroid tumors frequently harbor *BRAF* and *RAS* (*N*-, *H*- and *K*-) proto-oncogene-activating mutations,[3,4] which constitutively turn on the mitogen-activated protein kinase (MAPK) signaling pathway, leading to abnormal cell growth and survival. In the thyroid, the output intensity of the MAPK signal negatively regulates the expression of key genes involved in RAI uptake and retention.[5,6] This in combination with other undefined factors can transform thyroid tumors into highly aggressive RAI-resistant entities.

The first stage of The Cancer Genome Atlas Project (TCGA) comprehensively described the genomic landscape of the most prevalent DTC histotype, papillary thyroid carcinoma (PTC).[7] However, patient follow-up was restricted and the most aggressive histopathologies were excluded, limiting the identification of molecular events with prognostic value. Later studies of RAI-refractory-enriched carcinoma series identified genetic hallmarks associated with tumor virulence.[3,4] Still, there are genomic traits barely explored for poor outcome tumors. MiRNome profiling has uncovered markers associated with specific clinicopathological features for many cancer types, including thyroid cancer.[8,9] Identification of their direct targets has led to deciphering their functional effects and their promise as therapeutic targets.[10,11]

Here, we sequenced the miRNome of a long-term follow-up thyroid cancer series enriched with poor prognosis cases and found hsa-miR139-5p downregulation as a *bona fide* poor-prognostic factor. Exogenous hsa-miR-139-5p expression repressed procancer features of thyroid cancer (TC) cells. Proteomic analysis revealed that the alternative splicing factor HNRNPF was significantly regulated by hsa-miR-139-5p. Subsequent RNA sequencing analysis showed that the modulation of hsa-miR-139-5p/HNRNPF axis affected alternative splicing outcome of genes related to MAPK and PI3K signaling cascades. The axis represents a novel putative mechanism of regulation of key cancer pathways.

Materials and Methods

Human thyroid tissues

A total of 49 fresh frozen-thyroid tissues including 25 carcinomas from patients with aggressive disease (8 differentiated thyroid carcinomas from persistent/recurrent disease patients, 2 lymphadenopathies from a papillary thyroid carcinoma, 5 poorly differentiated carcinomas and 10 anaplastic thyroid cancers), 17 carcinomas from disease-free patients, 4 benign tumors (follicular adenomas [FAs]) and 3 normal thyroids (NTs) from patients with non-thyroid pathologies were analyzed by miRNome sequencing. Associated clinicopathologic data are detailed in Supporting Information Table S1. Formalin-fixed paraffin-embedded (FFPE) tissue sections of local metastases from 14 patients were also collected. Triplets of normal, primary tumor and local metastasis were available for 7 of these 14 patients. Frozen and FFPE specimens were first evaluated by a pathologist. All tumors included in the study held a tumor content superior to 80%.

Cell lines

CAL-62 (RRID:CVCL_1112) and 8505C (RRID:CVCL_1054) cell lines derived from human anaplastic thyroid carcinomas were kindly provided by Dr. JA Fagin (MSKCC, NY). Both cell lines were mycoplasma-free and authenticated by an STR-based method within the last 3 years at the CNIO Genomics Unit.

Their respective driver mutations (CAL-62: $KRAS^{G12R}$ and 8505C: $BRAF^{V600E}$) were confirmed by Sanger sequencing. Cells were maintained at 37°C and 5% CO_2 in a humidified atmosphere and grown in RPMI-1640 growth medium (Sigma) supplemented with 10% (v/v) Fetal Bovine Serum (FBS; Sigma, St. Louis, MO). CAL-62 isogenic cell lines expressing either mature hsa-miR-139-5p or a nontargeting control under a doxycycline-inducible promoter were established following the manufacturer's protocol (Dharmacon, shmimic-inducible-manual). Briefly, CAL-62 cells were infected with lentiviral particles containing either shMIMIC inducible hsa-miR-139-5p mCMV-Turbo GFP vector (P_{TRE3G}-tGFP-hsa-miR139-5p, Dharmacon VSH6904-224633476) or SMARTvector inducible nontargeting control mCMV-Turbo GFP vector (P_{TRE3G}-tGFP-nontargeting control, Dharmacon VSC11651). These systems also encode the Tet-On® 3G transactivator protein, which expression is under the control of a constitutive RNA pol II promoter. Both hsa-miR-139-5p or nontargeting control expression and GFP expression are regulated by the Tet 3G promoter, which is activated by the Tet-On® 3G transactivator only in the presence of doxycycline. The induction of GFP signal upon doxycycline treatment was monitored with a fluorescence microscope (Nikon Eclipse Ti-U). Hsa-miR-139-5p expression was quantified by Q-PCR at experiment end-points as experiment control.

Study approval

Tumors and normal thyroid tissues were collected from the Hospitals 12 de Octubre, Móstoles, La Paz, Vall d'Hebron, Germans Trias i Pujol and the CNIO Tumor bank with the approval of the respective institutional review boards and Bioethics and animal welfare committee of the Carlos III Health Institute. Patients completed a written informed consent prior to inclusion in the study.

Statistical information

General statistical analyses were conducted using Fisher's exact test for categorical variables, and a two-tailed *t*-test for continuous variables (GraphPad Prism v5.03 and SPSS v19). Relapse/death-free survival rates (Supporting Information Table S1) were calculated by the Kaplan–Meier test, and log-rank tests were used to examine the differences in disease-free survival rates between the two groups. Pearson's χ^2 test was used to analyze the associations of hsa-miR-139-5p expression with indicated clinicopathological variables. Values of $p \leq 0.05$ were considered as statistically significant.

Data availability

The human samples miRNome sequencing data and CAL-62 RNA sequencing data are deposited in the Gene Expression Omnibus (GEO) and are accessible through accession number GSE124653 and GSE123680, respectively. The proteomic analysis data are deposited in EBI ProteomeXchange and are accessible through accession number PXD011901. The remaining data and methods are available within the article and Supporting Information files or from the authors upon request.

Results and Discussion

MiRNome profiling patterns correlate with specific molecular and clinicopathological features

To discover novel putative biomarkers associated with persistent or recurrent disease we sequenced the miRNome of a fresh-frozen thyroid tissue series including 3 normal tissues (NT), 4 adenomas (FA) and 42 carcinomas (Supporting Information Table S1). Unsupervised analysis clustered the tumors into two main groups, subdivided into a total of five subclusters (Fig. 1*a*). The subclusters were enriched with specific histotypes and molecular classes: Subcluster 1 compiled most dedifferentiated carcinomas (10/15 ATCs or PDTCs, $p < 0.0001$); Subcluster 2 gathered *BRAF*-mutant tumors (8/11 *BRAF*-mutant primary tumors, $p < 0.0001$); Subcluster 3 was enriched in the DTC histotype follicular thyroid carcinoma (5/8 FTCs, $p = 0.0074$); Subcluster 4 in *RAS*-mutant tumors (8/13 *RAS*-mutant, $p = 0.0002$); and Subcluster 5 compiled normal thyroids and tumors negative for *BRAF* and *RAS* mutations.

MiRNome profiles are conditioned by the stromal cell component of the tumor

Dedifferentiated TCs contain infiltrating inflammatory cells,[12] which can represent up to 50% of the tumor mass. These non-cancer cells are mainly tumor-associated macrophages (TAMs). TAMs represent a major constituent of the tumor microenvironment and support cancer cells in malignant processes such as invasion, metastasis and evasion of the immune response. This tumor component can affect miRNome profiles and may lead to a misinterpretation of the results. Hence, we decided to quantify stroma infiltration in our series, to determine the correlation of this trait with tumor cluster yielded by hierarchical miRNome analysis. We developed a stromal cell score (SCS), which summarize the expression of the stromal cell markers *CD68*, *CD163* and *CSFR1* (Supporting Information Table S2).

SCS score (Fig. 1*a*) showed a significant association with miRNome clustering (Subclusters 1–5; Kruskal–Wallis test, statistics = 27.93, $p < 0.0001$). Remarkably, Subcluster 2 assembled differentiated TCs with mainly positive SCS including all poor-prognosis *BRAF*-mutant TCs. SCS was consistently lower (median SCS = 0.84) in these tumors than in those from Subcluster 1 (median SCS = 2.14), suggesting that these differentiated carcinomas harbor molecularly detectable grades of stroma infiltration. The specificity of the SCS score was confirmed by assessing the noncancer cell component of selected tumors (Supporting Information Fig. S1*a*) by an independent approach (Supporting Information Figs. S1*b* and S1*c*).

Differential expression analysis of the miRNome reveals prognostic thyroid cancer markers

To discover putative prognostic biomarkers, we categorized tumors as persistent/recurrent disease-related or disease-free-related; the

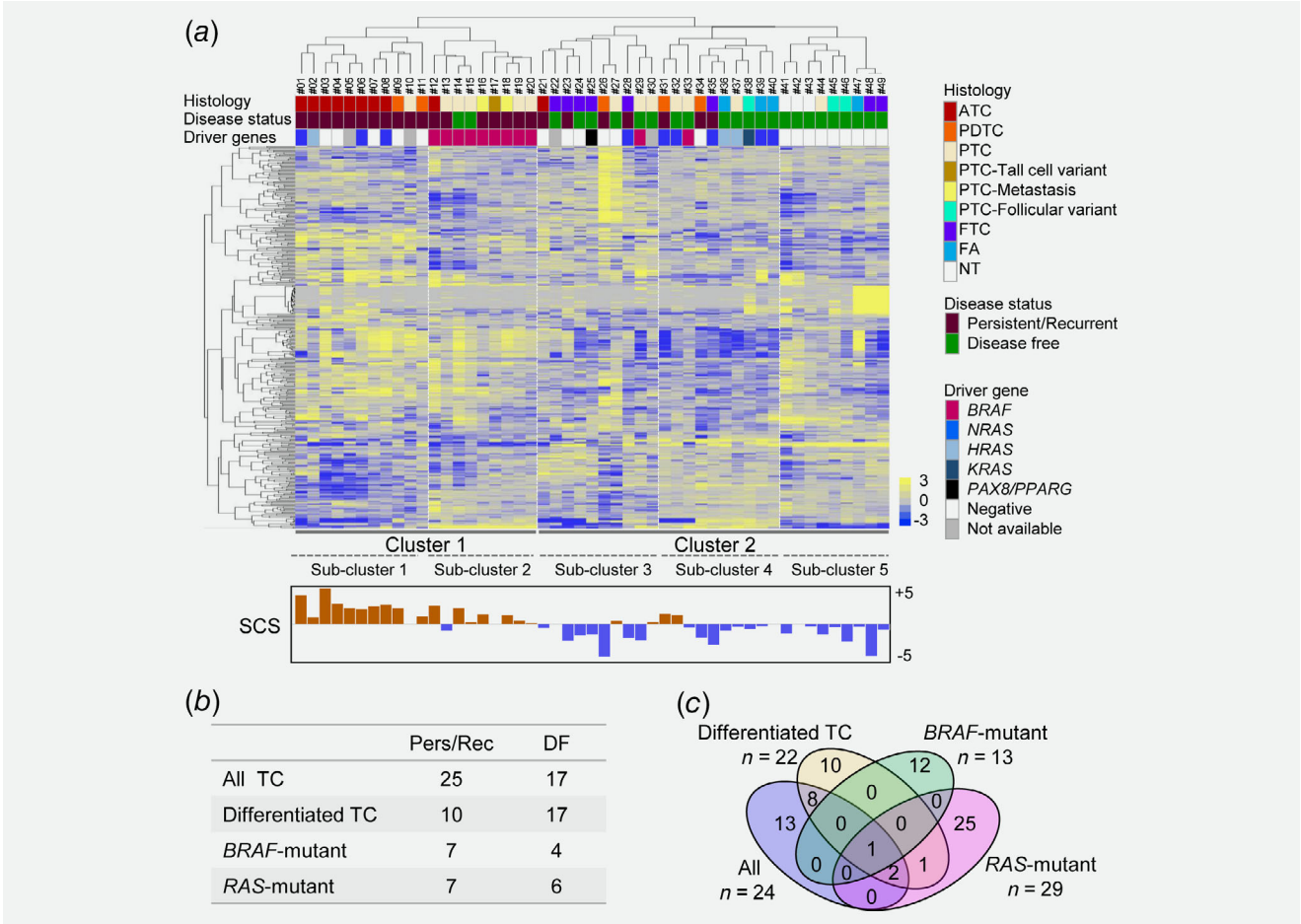

	Pers/Rec	DF
All TC	25	17
Differentiated TC	10	17
BRAF-mutant	7	4
RAS-mutant	7	6

Figure 1. MiRNome profiling analysis identifies potential persistent/recurrent disease biomarkers. (*a*) Hierarchical clustering analysis and miRNome heatmap for 49 thyroid tissues. Sample histology, disease status and tumor driver gene information are included. Stromal cell score (SCS) is shown below. Scale bars show log_2-normalized median-centered miRNA counts. (*b*) Number of patients included in miRNome differential expression analyses considering disease prognosis, histology and cancer driver gene. Abbreviation: DF, disease-free-related tumors with a median follow-up of 96 months. (*c*) Venn diagram of established comparisons of significant miRNAs.

latter category refers to tumors from disease-free patients with a median follow-up of 96 months (Fig. 1*a*, "Disease status," and Supporting Information Table S1). We performed differential expression analysis between the prognostic classes considering all thyroid carcinomas (all TCs), only DTCs, or only tumors from the same genetic class (*BRAF*-mutant, *RAS*-mutant; Fig. 1*b*). MiRNAs with an FDR value <0.1 and Log_2 Fold-change >1.5 or FDR value ≤0.05 were considered significantly differentially expressed. A total of 72 miRNAs passed the threshold for at least one of the comparisons (Supporting Information Table S3). Eleven miRNAs were significantly associated with prognosis for both "All TCs" and "DTCs" (Supporting Information Table S3), indicating that deregulation of these miRNAs was already present in less advanced histotypes, and thus pointing at them as putative prognostic biomarkers for earlier cancer stages. Among them, we found the upregulation of onco-miRNA hsa-miR-21-5p[13,14] and six miRNAs encoded by the 14q32 region, which contains two miRNA clusters located within an imprinted *locus*.[15] Remarkably, the upregulation of these miRNA clusters has been previously associated with poor outcome disease in other solid tumors.[16,17]

Twenty nine miRNAs were associated with the prognosis of *RAS*-mutant tumors (Supporting Information Table S3 and Fig. S2*a*). These miRNAs hold special clinical interest since *RAS*-mutations occur in benign tumors (FAs), DTCs (FTCs and PTC follicular variant) and dedifferentiated carcinomas, and thus their quantification could facilitate discrimination between these entities at diagnosis and anticipate the outcome of early-stage *RAS*-mutant cancers. MiRNAs showing a significant correlation with SCS score were considered stroma infiltration markers rather than *bona fide* prognostic factors (Supporting Information Figs. S2*a* and S2*b*).

Hsa-miR139-5p is downregulated in persistent/recurrent disease-related primary tumors and local metastases

Hsa-miR-139-5p was the only miRNA that showed significant association with persistent/recurrent disease, independently of

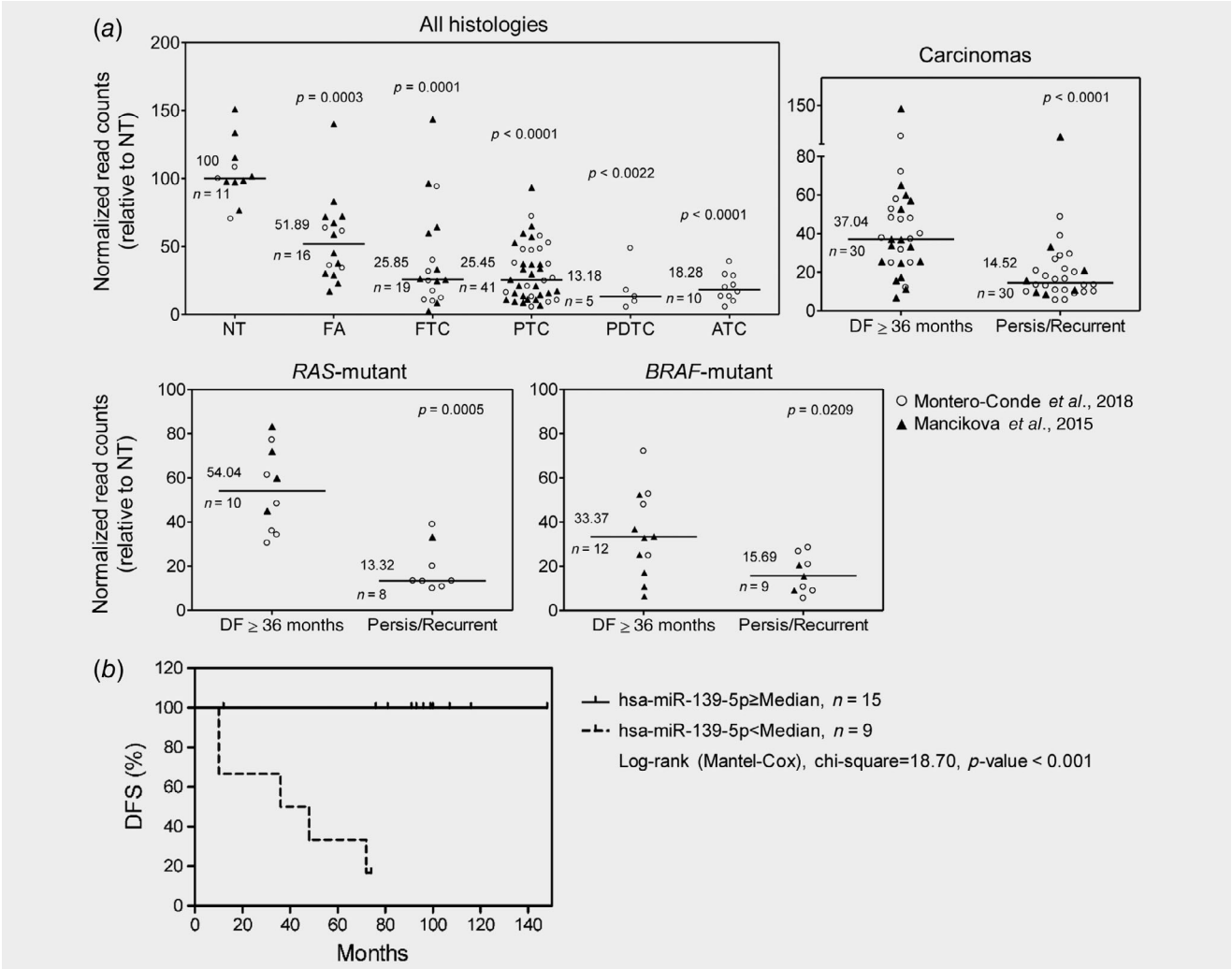

Figure 2. Hsa-miR-139-5p is a *bona fide* marker of persistent/recurrent disease in thyroid cancer. (*a*) Hsa-miR-139-5p $DESeq_2$-normalized read counts relative to median expression of normal thyroid sample series. Grand median values, sample size and Mann–Whitney *t*-test *p* values for indicated comparisons are shown. Abbreviations: DF, disease-free related tumors with a follow-up ≥36 months; Persis/Recurrent, persistent/recurrent related disease tumors. (*b*) Kaplan–Meier disease-free survival (DFS) plot. Hsa-miR-139-5p median expression value of miRNome-seq primary carcinomas was used to separate DTC patients into two groups: low expressors (dashed line) and high expressors (solid line).

the genetic background and stroma-component/tumor dedifferentiation stage (Fig. 1*c* and Supporting Information Table S3). In addition, we evaluated the clinicopathological variables in thyroid cancer to determine the clinical relevance of hsa-miR-139-5p expression. A significant association of hsa-miR-139-5p with age at diagnosis (Pearson's $\chi^2 = 8.046$, *p*-value = 0.005), lymph node metastasis (Pearson's $\chi^2 = 9.079$, *p*-value = 0.003) and TNM stage (AJCC 8th edition; Pearson's $\chi^2 = 20.501$, $p < 0.001$) was observed (Supporting Information Table S4).

Downregulation of this miRNA was previously described in TCs as compared to benign tumors or normal thyroids,[9,18,19] and has been proposed as a marker of diagnosis and aggressive disease in multiple cancer types.[20–22] To determine if hsa-miR-139-5p downregulation was detectable in early stages of thyroid tumor development, we enriched our series with the Mancikova *et al.* series.[8] Hsa-miR-139-5p analysis showed a gradual reduction of its abundance from normal thyroid to FA ($p = 0.0003$), DTC ($p = 0.0001$ for FTCs and $p < 0.0001$ for PTCs) and dedifferentiated carcinomas ($p = 0.0022$ for PDTCs and $p = 0.0001$ for ATCs; Fig. 2*a*). Prognosis-associated significant differences were also detected for both series considering only DTCs ($p < 0.0001$), *BRAF*-mutant ($p = 0.0209$) or *RAS*-mutant ($p = 0.0005$) tumors (Fig. 2*a*). Furthermore, we validated hsa-miR-139-5p downregulation in the thyroid cancer TCGA series.[7] Hsa-miR-139-5p was significantly downregulated in the persistent disease tumor class, independently of the genetic background (either

BRAF-mutant or *RAS*-mutant; Supporting Information Fig. S3*a*). Disease-free survival (DFS) analysis showed significant differences in the time to relapse or death between hsa-miR-139-5p high-expressors and low-expressors DTC patients (Supporting Information Table S1 and Fig. 2*b*).

Finally, we evaluated hsa-miR-139-5p expression in 15 lymph node metastases of 14 patients with DTC. Normal thyroid tissue, primary tumor and metastases triplets were available for 6 of the 11 persistent/recurrent disease patients and a disease-free patient with a short follow-up (17 months) and an

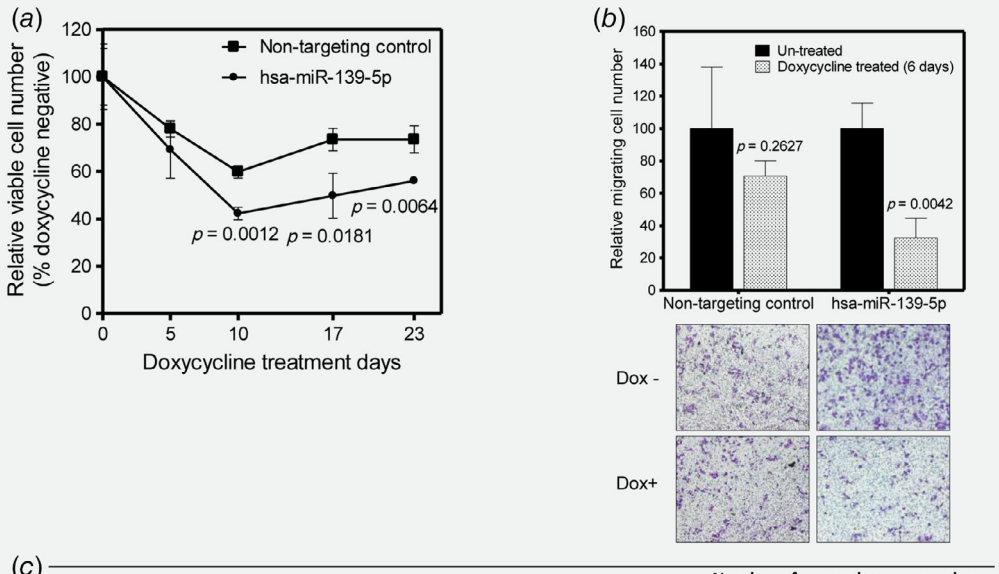

(c)

Protein	Gene	Function	Condition	Log_2 ratio	Number of spectra	*p*-value ratio	*p*-value sample
P52597	***HNRNPF***	Alternative splicing factor	96 hr	−0.45	40	0.0123	0.0122
			120 hr	−0.52	41	0.0112	0.0079
Q6R327	***RICTOR***	mTOR complex 2 subunit, mTOR signaling pathway	96 hr	−0.31	9	0.0367	0.0485
			120 hr	−0.31	8	0.0003	0.0380
P84022; Q15796	***SMAD3; SMAD2***	TGF-beta signaling transducers and transcriptional modulators.	96 hr	−0.37	4	0.0293	0.0298
			120 hr	−0.61	4	0.0016	0.0086
P19021	***PAM***	Peptidylglycine alpha-amidating monooxygenase.	96 hr	−0.71	2	0.0433	0.0035
			120 hr	−0.88	2	0.0181	0.0019

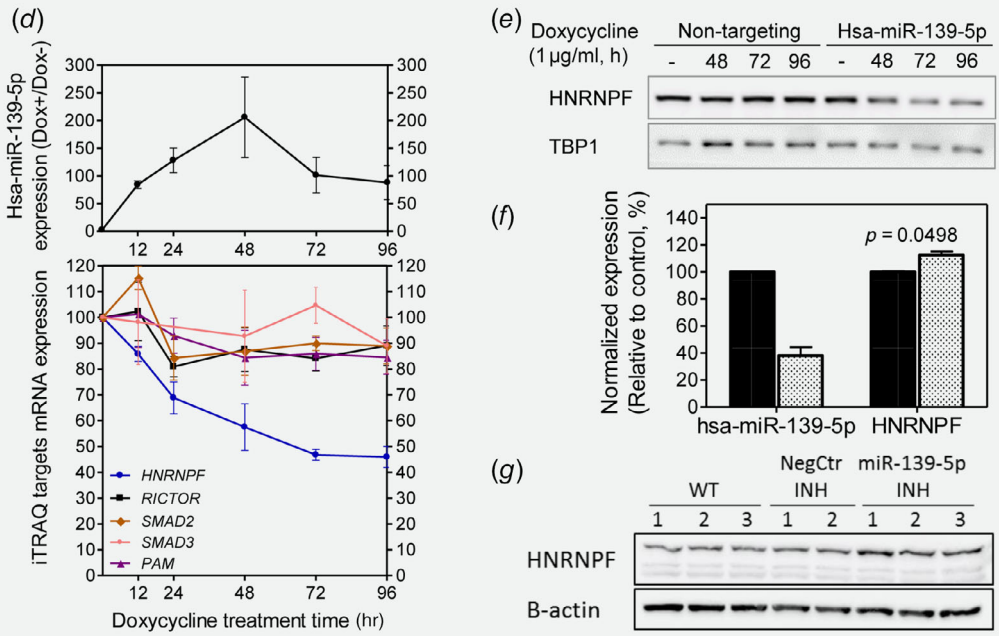

Figure 3. Legend on next page.

aggressive histology (tall cell PTC). As in primary tumors, hsa-miR-139-5p was significantly downregulated in the metastases from poor prognosis patients compared to those from disease-free patients (≥91 months follow-up; $p = 0.0364$; Supporting Information Fig. S3*b*, left panel), and the magnitude of deregulation was comparable in primary tumor and paired metastasis (Supporting Information Fig. S3*b*, right panel). Altogether, these findings discard hsa-miR-139-5p downregulation as a passenger aberration, and suggest that this miRNA has a functional role in early acquisition stages of virulent attributes.

In vitro induction of hsa-miR-139-5p expression inhibits cell proliferation and migration

To explore if hsa-miR-139-5p expression could inhibit procancer features in thyroid cancer cells, we selected the *RAS*-mutant anaplastic cancer cell line CAL-62, with an almost undetectable hsa-miR-139-5p expression, and established a cell line with a doxycycline-dependent expression of the mature miRNA and a second one with a doxycycline-dependent expression of a nontargeting sequence. Induction of hsa-miR-139-5p expression in CAL-62 significantly inhibited cell proliferation compared to nontargeting control cells, as shown by counting the viable cells (Fig. 3*a*). However, cell proliferation reduction did not reach 25%, suggesting a minor effect of hsa-miR-139-5p on cell proliferation in thyroid cancer. Conversely, a transwell migration assay showed that induction of hsa-miR-139-5p expression inhibited cell migration to almost 40% (p-value = 0.0127) of the nontargeting control condition (Fig. 3*b*), indicating that cells with low hsa-miR-139-5p expression have a migratory advantage. Similar results were observed by scratch assay (Supporting Information Fig. S5).

Hsa-miR-139-5p regulates the expression of proteins related to poor-survival cancer

To identify hsa-miR-139-5p-regulated genes related to previously observed phenotypic changes, we measured hsa-miR-139-5p regulatory output with an unbiased strategy able to detect both miRNA–mRNA destabilized targets and miRNA translation-inhibited targets. We used the quantitative mass spectrometry (LC–MS/MS)-based technique isobaric tags for relative and absolute quantitation (iTRAQ)[23] to detect proteomics differences upon induction of hsa-miR-139-5p expression in CAL-62 cell line. A total of 6,139 proteins were identified. We observed a significant differential expression (Log_2 ratio >0.3 or <−0.3; p-value <0.05) for 71 proteins at 96 hr hsa-miR-139-5p expression induction, and 50 proteins at 120 hr induction with an overlap of 12 proteins between the two time points (Supporting Information Table S5). We reasoned that protein abundance kinetics of true miRNA-targets should display a significant decrease at 96 hr being sustained or more acute at 120 hr (log_2 ratio at 120 hr ≤ log_2 ratio at 96 hr). Among proteins fitting these criteria, we found RICTOR, SMAD2/3, HNRNPF and PAM (Fig. 3*c* and Supporting Information Table S5). Notably, quantification of RICTOR, SMAD2/3 and HNRNPF protein level was based on the measurement of multiple peptides (i.e., number of spectra; Supporting Information Table S5), which confers robustness to the findings (Fig. 3*c*). These candidates are key proteins in the cancer-related pathways/processes mTOR2/AKT, TGFbeta and alternative splicing, respectively, and their expression has been shown to mediate poor outcome[24,25] and resistance to therapy[26] in different cancer types including thyroid cancer.[27–29]

We used TargetScan version 7.0[30] to search for hsa-miR-139-5p-matched sites within the 3'UTR sequence of the candidate genes and found one 7 mer-seed matched-site for each of them (Supporting Information Fig. S4*a*). The *HNRNPF* site showed the highest probability value (P_{CT}) of being selectively conserved rather than by chance. Q-PCR analysis indicated that *HNRNPF* mRNA abundance was acutely reduced upon hsa-miR-139-5p expression induction ($r = -0.9364$, $p = 0.0059$), showing a maximal reduction of 54% at 96 hr (Fig. 3*d*); this was validated by western blot (Fig. 3*e*). Conversely, *HNRNPF* mRNA and protein abundance exhibited a modest but consistent increase when endogenous hsa-miR-139-5p expression was inhibited with a hsa-miR-139-5p hairpin inhibitor in a thyroid cancer cell line (8505C) with detectable expression of the miRNA as compared to the nontargeting control condition (Figs. 3*f* and 3*g*).

Finally, we analyzed the expression of *HNRNPF* in our tumor series. Correlation analysis of *HNRNPF* mRNA abundance and hsa-miR-139-5p expression revealed a significant inverse association (Pearson $r = -0.3258$, $p = 0.0290$; Supporting Information Fig. S4*b*), which was also significant for the papillary thyroid cancer

Figure 3. Exogenous hsa-miR-139-5p expression inhibits procancer features and regulates proteins involved in known cancer-related pathways. (*a*) Viable cell number of CAL-62 doxycycline-inducible hsa-miR-139-5p and nontargeting control cell lines at indicated days of doxycycline treatment (1 μg/ml). Data were represented as relative to the untreated condition (doxycycline treatment days = 0). Differences between cell lines for each time point were estimated by *t*-test; significant *p* values are shown. (*b*) Percentage of migrating cells of nontargeting control and hsa-miR-139-5p inducible cells for indicated conditions. Differences were estimated by *t*-test. Abbreviation: Dox: Doxycycline. Images of representative microscope fields (10×) for each experimental condition are shown. Abbreviation: Dox −/+: doxycycline untreated/treated. (*c*) Protein levels for hsa-miR-139-5p potential targets as determined by LC–MS/MS using iTRAQ. (*d*) Abundance kinetics of hsa-miR-139-5p (upper panel) and mRNAs of iTRAQ top-candidates (lower panel) for hsa-miR-139-5p inducible cells treated with doxycycline for indicated times. Data is represented relative to doxycycline untreated condition. (*e*) Immunoblot of HNRNPF protein from nuclear extracts of nontargeting control and hsa-miR-139-5p inducible cells treated with doxycycline for indicated times. TBP1 was used as loading control. (*f*) Hsa-miR-139-5p and *HNRNPF* mRNA abundance in 8505C cells transfected either with a nontargeting control inhibitor (black bar) or hsa-miR-139-5p hairpin inhibitor (white bar). Bars represent means ± SD of three independent transfection experiments each measured in triplicate. (*g*) Immunoblot of HNRNPF protein from total protein extracts of 8505C cells at different conditions: untransfected (wt), 72 hr posttransfection with a negative control inhibitor (Neg Ctr INH) or 72 hr posttransfection with the hsa-miR-139-5p inhibitor (hsa-miR-139-5p INH). Replicates of each experimental condition were included. β-Actin was used as loading control.

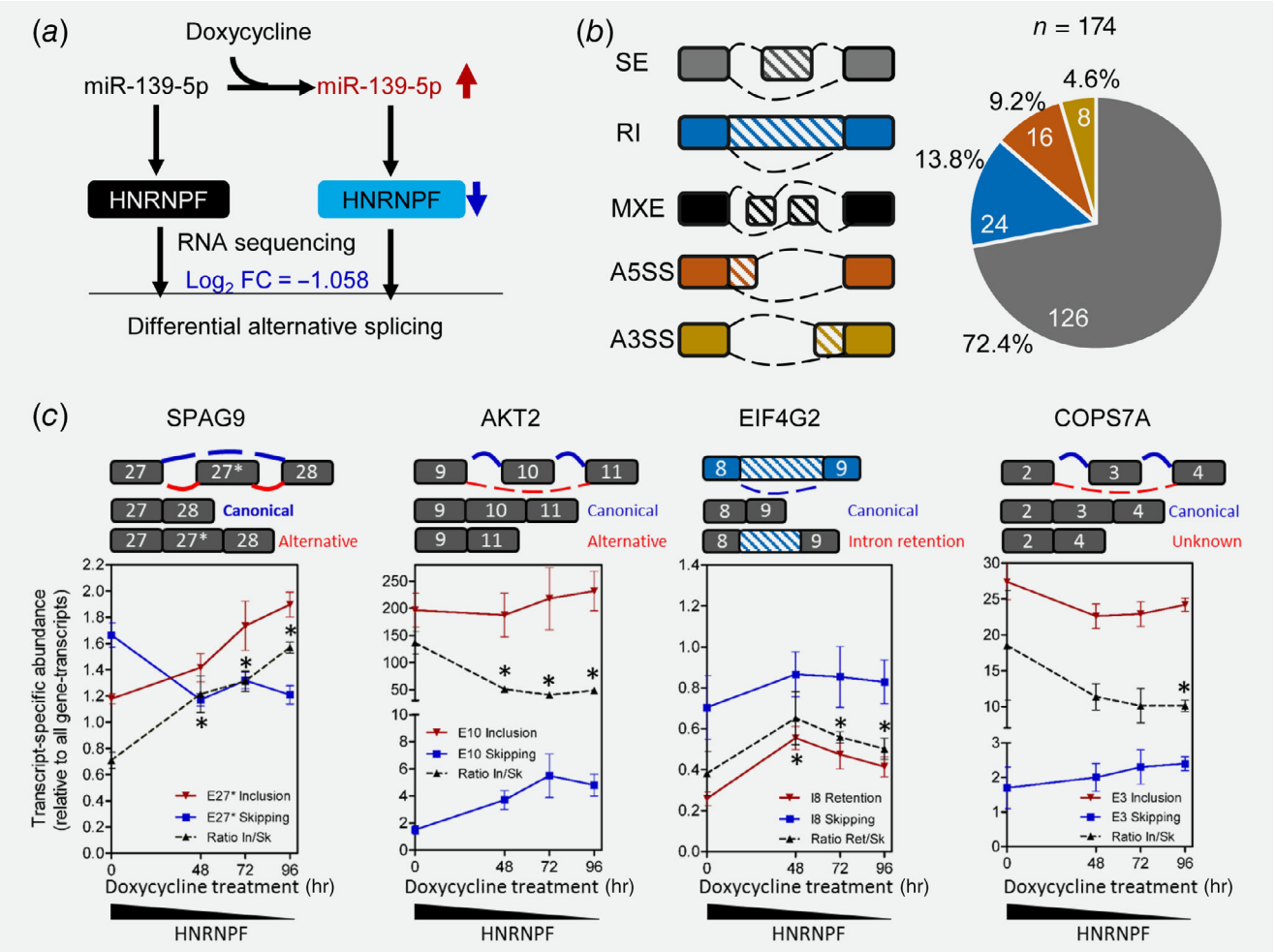

Figure 4. Hsa-miR-139-5p/HNRNPF regulatory axis modulates gene-transcripts balance. (*a*) Workflow of alternative splicing analysis experiment. Log_2 FC = −1.058 refers to $DESeq_2$ differential expression analysis of *HNRNPF* upon hsa-miR-139-5p expression induction. rMATS was used to identify differences in splicing. (*b*) Pie chart of events with significantly different inclusion levels (FDR < 0.05) upon hsa-miR-139-5p/HNRNPF axis regulation. Junction counts and reads on target exon counts from RNA sequencing data were considered in the analysis. Abbreviations: SE, skipped exon; RI, retained intron; MXE, mutually exclusive; A5SS, alternative 5′ splice site; A3SS, alternative 3′ splice site. (*c*) Q-PCR validation of hsa-miR-139-5p/HNRNPF regulated alternative splicing events for indicated genes. Graphic schemes of the exons/introns involved in each event are included. Blue color represents event outcomes corresponding to the canonical protein-coding transcript; red color represents event outcomes corresponding to either an alternative protein-coding (alternative), intron-retained or unknown transcript. Connecting lines represent the kinetics of the specific isoforms (canonical in blue and alternative in red) and exon/intron inclusion/skipping ratios (black dashed line) upon HNRNPF inhibition. Error bars represent SD of each time point (0, 48, 72 and 96 hr) measured in quadruplicate. Mann–Whitney *t*-test between 48 hr, 72 hr, 96 hr and basal condition (0 hr) was performed. *$p \leq 0.05$.
[a]SPAG9-event was previously described in 293T cells.[32]

TCGA series and other cancer types, as observed by the starBase Pan-Cancer analysis platform[31] (Supporting Information Fig. S4*c*).

The hsa-miR-139-5p/HNRNPF axis modulates gene-transcripts balance

HNRNPF is an alternative splicing factor with a major role in cryptic exons inclusion/exclusion.[32] It has been reported to mediate the alternative splicing of multiple genes involved in different cancer-related processes, such as the epithelial to mesenchymal transition[33] and resistance to therapy.[26] Recent reports have shown that the activity of alternative splicing regulators is recurrently altered in cancer,[4,34–37] and this affects transcripts balance of key genes involved in cancer-related pathways.[26,33,38]

To explore the alternative splicing changes upon hsa-miR-139-5p/HNRNPF axis regulation, we performed an RNA-sequencing assay with the established CAL-62 isogenic cell lines expressing either mature hsa-miR-139-5p or a nontargeting control under a doxycycline-inducible promoter, and used the Multivariate Analysis of Transcript Splicing (rMATS) computational tool to analyze the data (Fig. 4*a*). Differential analysis of major splicing events outcomes between untreated

and doxycycline-treated condition for both cell lines revealed 174 events significantly activated or repressed (FDR < 0.05) only upon hsa-miR-139-5p expression induction (Fig. 4*b* and Supporting Information Table S6). Exon skipping was the most frequent event, as previously reported[32] (Fig. 4*b*). In concordance with a pre-mRNA processing regulation mechanism, affected genes only showed significant differences in the abundance of splicing event outcomes (Supporting Information Table S6*a*) but not in the merged transcript abundance (Supporting Information Table S6*b*). "Skipped exon" and "retained intron" events occurred in genes related to thyroid cancer signaling cascades RTK/RAS/MAPK (*KSR1*, *MAPK12*, *SPAG9*) and PI3K/AKT/mTOR (*PI4KA*, *AKT2*, *MLST8, EIF4G2*; Supporting Information Table S6*a* and Fig. 4*c*); which could modulate pathway outputs. Finally, we validated by Q-PCR several of the identified events, which further supports the rMATS analysis results (Fig. 4*c*).

In summary, miRnome profiles of thyroid tumors correlate with tumor histopathology and tumor driver gene, highlighting the clinical potential of miRnome profiling to classify patients according to certain clinicopathological features. Moreover, miRnome differential expression analysis between prognostic classes identify hsa-miR-139-5p as a disease outcome marker and, although the current size of the series is limiting, hsa-miR-139-5p association with disease-free survival is clinically relevant and will be explored across a larger series. Notably, we find that this molecule regulates the abundance of the alternative splicing factor HNRNPF and further observe that hsa-miR-139-5p/HNRNPF expression modulates the transcript balance of genes involved in key cancer-related signaling pathways. Hence, our data point to this new mechanism as a modulator of these pathways outputs, and, consequently, tumor virulence, which could be applied to other cancers.

Acknowledgements

This work was supported by Project PI14/00240, PI17/01796 [Instituto de Salud Carlos III (ISCIII), Acción Estratégica en Salud, cofinanciado a través del Fondo Europeo de Desarrollo Regional (FEDER)], and CAM (S2017/BMD-3724; TIRONET2-CM). CMC is supported by a grant from the AECC Foundation (AIO15152858 MONT). We thank the Genomics Core Unit at the CNIO for generating miRNome and RNA-seq libraries, the Spanish National Tumor Bank Network (RD09/0076/00047) for the support in obtaining tumor samples, and all patients, physicians, and tumor biobanks involved in the study.

References

1. Nixon IJ, Whitcher MM, Palmer FL, et al. The impact of distant metastases at presentation on prognosis in patients with differentiated carcinoma of the thyroid gland. *Thyroid* 2012;22:884–9.
2. Smallridge RC, Marlow LA, Copland JA. Anaplastic thyroid cancer: molecular pathogenesis and emerging therapies. *Endocr Relat Cancer* 2009;16:17–44.
3. Landa I, Ganly I, Chan TA, et al. Frequent somatic TERT promoter mutations in thyroid cancer: higher prevalence in advanced forms of the disease. *J Clin Endocrinol Metab* 2013;98:E1562–6.
4. Pozdeyev N, Gay LM, Sokol ES, et al. Genetic analysis of 779 advanced differentiated and anaplastic thyroid cancers. *Clin Cancer Res* 2018;24:3059–68.
5. Chakravarty D, Santos E, Ryder M, et al. Small-molecule MAPK inhibitors restore radioiodine incorporation in mouse thyroid cancers with conditional BRAF activation. *J Clin Invest* 2011;121:4700–11.
6. Ho AL, Grewal RK, Leboeuf R, et al. Selumetinib-enhanced radioiodine uptake in advanced thyroid cancer. *N Engl J Med* 2013;368:623–32.
7. Agrawal N, Akbani R, Aksoy BA, et al. Integrated genomic characterization of papillary thyroid carcinoma. *Cell* 2014;159:676–90.
8. Mancikova V, Castelblanco E, Pineiro-Yanez E, et al. MicroRNA deep-sequencing reveals master regulators of follicular and papillary thyroid tumors. *Mod Pathol* 2015;28:748–57.
9. Dettmer MS, Perren A, Moch H, et al. MicroRNA profile of poorly differentiated thyroid carcinomas: new diagnostic and prognostic insights. *J Mol Endocrinol* 2014;52:181–9.
10. Rupaimoole R, Slack FJ. MicroRNA therapeutics: towards a new era for the management of cancer and other diseases. *Nat Rev Drug Discov* 2017;16:203–22.
11. Tang W, Zhou W, Xiang L, et al. The p300/YY1/miR-500a-5p/HDAC2 signalling axis regulates cell proliferation in human colorectal cancer. *Nat Commun* 2019;10:663.
12. French JD, Bible K, Spitzweg C, et al. Leveraging the immune system to treat advanced thyroid cancers. *Lancet Diabetes Endocrinol* 2017;5:469–81.
13. Sondermann A, Andreghetto FM, Moulatlet ACB, et al. MiR-9 and miR-21 as prognostic biomarkers for recurrence in papillary thyroid cancer. *Clin Exp Metastasis* 2015;32:521–30.
14. Guo Z, Hardin H, Montemayor-Garcia C, et al. In situ hybridization analysis of miR-146b-5p and miR-21 in thyroid nodules: diagnostic implications. *Endocr Pathol* 2015;26:157–63.
15. Luk JM, Burchard J, Zhang C, et al. DLK1-DIO3 genomic imprinted MicroRNA cluster at 14q32.2 defines a stemlike subtype of hepatocellular carcinoma associated with poor survival. *J Biol Chem* 2011;286:30706–13.
16. Nadal E, Zhong J, Lin J, et al. A MicroRNA cluster at 14q32 drives aggressive lung adenocarcinoma. *Clin Cancer Res* 2014;20:3107–17.
17. González-Vallinas M, Rodríguez-Paredes M, Albrecht M, et al. Epigenetically regulated chromosome 14q32 miRNA cluster induces metastasis and predicts poor prognosis in lung adenocarcinoma patients. *Mol Cancer Res* 2018;16:390–402.
18. Ye Y, Zhuang J, Wang G, et al. MicroRNA-139 targets fibronectin 1 to inhibit papillary thyroid carcinoma progression. *Oncol Lett* 2017;14:7799–806.
19. Chi J, Zheng X, Gao M, et al. Integrated microRNA-mRNA analyses of distinct expression profiles in follicular thyroid tumors. *Oncol Lett* 2017;14:7153–60.
20. Song C-J, Chen H, Chen L-Z, et al. The potential of microRNAs as human prostate cancer biomarkers: a meta-analysis of related studies. *J Cell Biochem* 2018;119:2763–86.
21. Ratert N, Meyer H-A, Jung M, et al. miRNA profiling identifies candidate miRNAs for bladder cancer diagnosis and clinical outcome. *J Mol Diagn* 2013;15:695–705.
22. Krishnan K, Steptoe AL, Martin HC, et al. miR-139-5p is a regulator of metastatic pathways in breast cancer. *RNA* 2013;19:1767–80.
23. Ross PL, Huang YN, Marchese JN, et al. Multiplexed protein quantitation in *Saccharomyces cerevisiae* using amine-reactive isobaric tagging reagents. *Mol Cell Proteomics* 2004;3:1154–69.
24. Li N, Xue W, Yuan H, et al. AKT-mediated stabilization of histone methyltransferase WHSC1 promotes prostate cancer metastasis. *J Clin Invest* 2017;127:1284–302.
25. González-González A, Muñoz-Muela E, Marchal JA, et al. Activating transcription factor 4 modulates TGFβ-induced aggressiveness in triple-negative breast cancer via SMAD2/3/4 and mTORC2 Signaling. *Clin Cancer Res* 2018;24:5697–709.
26. Fan L, Zhang F, Xu S, et al. Histone demethylase JMJD1A promotes alternative splicing of AR variant 7 (AR-V7) in prostate cancer cells. *Proc Natl Acad Sci USA* 2018;115:E4584–93.
27. Knauf JA, Sartor MA, Medvedovic M, et al. Progression of BRAF-induced thyroid cancer is associated with epithelial–mesenchymal transition requiring concomitant MAP kinase and TGFβ signaling. *Oncogene* 2011;30:3153–62.
28. Riesco-Eizaguirre G, Rodriguez I, De la Vieja A, et al. The BRAFV600E oncogene induces transforming growth factor secretion leading to sodium iodide Symporter repression and increased

malignancy in thyroid cancer. *Cancer Res* 2009;69: 8317–25.
29. Miller KA, Yeager N, Baker K, et al. Oncogenic Kras requires simultaneous PI3K Signaling to induce ERK activation and transform thyroid epithelial cells in vivo. *Cancer Res* 2009;69: 3689–94.
30. Agarwal V, Bell GW, Nam J-W, et al. Predicting effective microRNA target sites in mammalian mRNAs. *Elife* 2015;4:e05005.
31. Li J-H, Liu S, Zhou H, et al. starBase v2.0: decoding miRNA-ceRNA, miRNA-ncRNA and protein–RNA interaction networks from large-scale CLIP-Seq data. *Nucleic Acids Res* 2014;42: D92–7.
32. Huelga SC, Vu AQ, Arnold JD, et al. Integrative genome-wide analysis reveals cooperative regulation of alternative splicing by hnRNP proteins. *Cell Rep* 2012;1:167–78.
33. Huang H, Zhang J, Harvey SE, et al. RNA G-quadruplex secondary structure promotes alternative splicing via the RNA-binding protein hnRNPF. *Genes Dev* 2017;31:2296–309.
34. Seiler M, Peng S, Agrawal AA, et al. Somatic mutational landscape of splicing factor genes and their functional consequences across 33 cancer types. *Cell Rep* 2018;23:282–296.e4.
35. Sebestyén E, Singh B, Miñana B, et al. Corrigendum: large-scale analysis of genome and transcriptome alterations in multiple tumors unveils novel cancer-relevant splicing networks. *Genome Res* 2018;28:1426–6.
36. Ibrahimpasic T, Xu B, Landa I, et al. Genomic alterations in fatal forms of non-anaplastic thyroid cancer: identification of MED12 and RBM10 as novel thyroid cancer genes associated with tumor virulence. *Clin Cancer Res* 2017;23:5970–80.
37. Kahles A, Lehmann K-V, Toussaint NC, et al. Comprehensive analysis of alternative splicing across Tumors from 8,705 patients. *Cancer Cell* 2018;34:211–224.e6.
38. Bechara EG, Sebestyén E, Bernardis I, et al. RBM5, 6, and 10 differentially regulate NUMB alternative splicing to control cancer cell proliferation. *Mol Cell* 2013;52:720–33.